Million-Atom Pseudopotential Calculation of Γ-X Mixing in GaAs/AlAs Superlattices and Quantum Dots

Lin-Wang Wang, Alberto Franceschetti, and Alex Zunger
National Renewable Energy Laboratory, Golden, Colorado 80401
(Received 1 November 1996)

We have developed a "linear combination of bulk bands" method that permits atomistic, pseudopotential electronic structure calculations for $\sim 10^6$ atom nanostructures. Application to $(GaAs)_n/(AlAs)_n$ (001) superlattices (SL's) reveals even-odd oscillations in the Γ-X coupling magnitude $V_{\Gamma X}(n)$, which vanishes for n = odd, even for *abrupt* and *segregated* SL's, respectively. Surprisingly, in contrast with recent expectations, 0D quantum dots are found here to have a *smaller* Γ-X coupling than equivalent 2D SL's. Our analysis shows that for large quantum dots this is largely due to the existence of level repulsion from *many* X states. [S0031-9007(97)02839-1]

PACS numbers: 73.20.Dx, 71.15.Hx, 73.61.Ey

The crossover from direct band gap to indirect band gap (e.g., $\Gamma \rightarrow X$) as a function of an external parameter is common in semiconductor physics. It is seen in (i) zinc blende materials (GaAs [1], InP [2]) as a function of pressure, (ii) alloys ($Al_xGa_{1-x}As$ [3], $Ga_xIn_{1-x}P$ [4]) as a function of composition x, and (iii) in superlattices (SL's) [5–9] and quantum dots [10,11] as a function of size or external pressure. While in cases (i) and (ii) the transition is believed to be first order [3], in nanostructures [case (iii)] the lack of translational invariances causes a quantum-mechanical mixing between the zone center Γ and the zone edge X states [12], measured by the coupling matrix element $V_{\Gamma X}$. Although small in magnitude ($V_{\Gamma X} \sim 10$ meV), the Γ-X coupling has profound consequences on the properties of the system, leading, for example, to the appearance of indirect transitions without phonon intervention [7,8], to characteristic pressure-induced changes of the photoluminescence intensity [9,10], to resonant tunneling in electronic transmission between GaAs quantum wells separated by an AlAs barrier [13] and to level splitting ("avoided crossing") in the pressure, electric-field, and magnetic-field induced Γ-X transition [5,6].

The significance of this small but crucial quantum-mechanical coupling has prompted attempts to measure $V_{\Gamma X}(m,n)$ in $(GaAs)_m/(AlAs)_n$ (001) superlattices, producing, however, widely scattered results: Meynadier *et al.* [5] found from the electric-field dependence of the photoluminescence energy $V_{\Gamma X}(12,28) = 1.25$ meV, while Pulsford *et al.* [6] found from the magnetic-field induced gap in the Landau level $V_{\Gamma X}(9,3) = 9$ meV. Measurements of the valence (v) to conduction (c) $\Gamma_v \leftrightarrow \Gamma_c$ and $\Gamma_v \leftrightarrow X_c$ emission [7] or absorption [8] fitted to theoretical models produced $V_{\Gamma X}(10,10) = 1.2$ meV in Ref. [7] and $V_{\Gamma X}(4,10) = 0.99$ meV in Ref. [8].

The calculation of $V_{\Gamma X}$ is difficult, as highlighted by the fact that the central approximation underlying the "standard model" of nanostructure physics–the conventional $\mathbf{k}\cdot\mathbf{p}$ model [14]—leads to $V_{\Gamma X} = 0$. Tight-binding [15,16], empirical pseudopotential [17–19], and first principles [20–22] calculations have been applied to abrupt, short-period superlattices, but are difficult to extend to lower symmetry structures such as quantum wires and dots or to interfacially rough superlattices. The interest in the latter systems stems from the recent suggestion [10] that $V_{\Gamma X}$ would exhibit a dramatic enhancement in zero-dimensional (0D) quantum dots relative to 2D periodic superlattices.

In this paper we introduce a method that permits direct and precise calculations of electronic structures, including the coupling $V_{\Gamma X}$, in large scale superlattices, wires, and dots. In analogy with the linear combination of atomic orbitals (LCAO) method, familiar in molecular chemistry, our "linear combination of bulk bands" (LCBB) method expands the states of the quantum structure in terms of the full-zone Bloch eigenstates of the constituent bulk solids. Like the $\mathbf{k}\cdot\mathbf{p}$ method [14], but unlike ordinary basis-set expansion approaches (tight-binding [15,16], plane waves [17–20]) the LCBB expansion allows for the selective inclusion of physically important (near edge) basis states, resulting in manageable Hamiltonian matrices that can be diagonalized with desktop computers even for million-(10^6) atom quantum structures. Unlike the conventional $\mathbf{k}\cdot\mathbf{p}$ method [14], however, intervalley (e.g., Γ-X) coupling and multiband mixing are fully included.

In conventional wave function expansion methods, the wave function $\psi_i(\mathbf{r})$ is expanded in terms of *fixed* basis functions (e.g., atomic orbitals or plane waves),

$$\psi_i(\mathbf{r}) = \sum_{\alpha=1}^{M} C_\alpha^{(i)}\, \phi_\alpha(\mathbf{r})\,. \tag{1}$$

Since the number M of basis functions $\phi_\alpha(\mathbf{r})$ scales linearly with the system size, such expansion becomes quickly impractical for large quantum nanostructures. The challenge of finding an accurate expansion with the smallest basis set requires *a physically motivated preselection of basis functions*, rather than a brute-force, systematic increase in the upper limit of Eq. (1).

This aspect of the problem is addressed in the $\mathbf{k}\cdot\mathbf{p}$ Luttinger-Kohn approach [14], where the zone-center

($\mathbf{k} = 0$) bulk Bloch functions $\{u_{n,0}\}$ are used to construct the basis functions $\phi_\alpha(\mathbf{r}) = u_{n,0}(\mathbf{r})\, e^{i\mathbf{k}\cdot\mathbf{r}}$. The wave function of the nanostructure is then expanded as

$$\psi_i(\mathbf{r}) = \sum_{n,\mathbf{k}} C^{(i)}_{n,\mathbf{k}} \left[u_{n,0}(\mathbf{r})\, e^{i\mathbf{k}\cdot\mathbf{r}}\right]. \tag{2}$$

The disadvantage of this approach is that it is unable to reproduce the band structure across the Brillouin zone; in particular, the bulk X_{1c} state is misplaced by >10 eV, as recently shown by Wood *et al.* [23,24], with the consequence that $V_{\Gamma X} \sim 0$ for all nanostructures.

The solution to this dilemma is to replace the zone-center states $\{u_{n,0}\}$ in Eq. (2) with the bulk Bloch states $\{u_{n,\mathbf{k}}\}$, leading to the linear combination of bulk bands method. For a periodic system consisting of materials A and B, Eq. (2) becomes

$$\psi_i(\mathbf{r}) = \sum_{\sigma=A,B} \sum_{n,\mathbf{k}}^{N_b,N_\mathbf{k}} C^{(i)}_{n,\mathbf{k},\boldsymbol{\sigma}} \left[u^\sigma_{n,\mathbf{k}}(\mathbf{r})\, e^{i\mathbf{k}\cdot\mathbf{r}}\right], \tag{3}$$

where the first sum runs over the constituent materials A and B, and the second sum runs over the bulk band index n and the supercell reciprocal lattice vectors $\mathbf{k}$ belonging to the first Brillouin zone of the underlying lattice. The advantage of the LCBB method over the conventional $\mathbf{k}\cdot\mathbf{p}$ method is that off-Γ states $u^\sigma_{n,\mathbf{k}\neq\mathbf{0}}$ of both materials can be directly included in the basis set, thus eliminating the need for hundreds of $\mathbf{k} = 0$ bulk states in the expansion of Eq. (2) to describe $k \gg 0$ states [23,24]. As a result, the bulk band structure is reproduced exactly in our approach, and the Γ-X coupling is naturally included without the need for an *ad hoc* treatment [25,26]. The advantage over Eq. (1) [15,16] is that the classification of the basis functions in terms of the band index n makes it intuitive to retain only the physically relevant band-edge states.

The Hamiltonian of the quantum structure has the form

$$\hat{H} = -\frac{\hbar^2}{2m}\nabla^2 + \sum_\alpha \sum_\mathbf{R} v_\alpha(\mathbf{r} - \mathbf{R} - \mathbf{d}_{\boldsymbol{\alpha}})\, W_\alpha(\mathbf{R}), \tag{4}$$

where the sum runs over the atomic types $\{\alpha\}$ and the primary cell positions $\{\mathbf{R}\}$. Here $v_\alpha(\mathbf{r})$ is the screened atomic pseudopotential for atom α and the weight function $W_\alpha(\mathbf{R})$ selects the atomic type at location $\mathbf{R}$. The Hamiltonian matrix elements in the LCBB representation are obtained by expanding the bulk Bloch functions $u^\sigma_{n,\mathbf{k}}(\mathbf{r})$ in a plane-wave basis set,

$$u^\sigma_{n,\mathbf{k}}(\mathbf{r}) = \sum_\mathbf{G}^{N_\mathbf{G}} B^\sigma_{n,\mathbf{k}}(\mathbf{G})\, e^{i\mathbf{G}\cdot\mathbf{r}}, \tag{5}$$

where the $N_\mathbf{G}$ coefficients $B^\sigma_{n,\mathbf{k}}(\mathbf{G})$ are calculated by diagonalizing the *bulk* Hamiltonian for each $\mathbf{k}$ point. The Bloch wave functions $u^\sigma_{n\mathbf{k}}$ are orthogonalized among different σ and n indexes at each $\mathbf{k}$ point to avoid overcompleteness. The Hamiltonian matrix elements are then

$$\langle\sigma'; n', \mathbf{k}'|\hat{H}|\sigma; n, \mathbf{k}\rangle = \Omega \sum_{\mathbf{G},\mathbf{G}'} B^{\sigma'}_{n',\mathbf{k}'}(\mathbf{G}') \left[\frac{\hbar^2}{2m}|\mathbf{k} + \mathbf{G}|^2 \delta_{\mathbf{k},\mathbf{k}'}\delta_{\mathbf{G},\mathbf{G}'} + \sum_\alpha v_\alpha(|\mathbf{k} + \mathbf{G} - \mathbf{k}' - \mathbf{G}'|) \times e^{-i\mathbf{d}_\alpha\cdot(\mathbf{k}+\mathbf{G}-\mathbf{k}'-\mathbf{G}')}\, W_\alpha(\mathbf{k} - \mathbf{k}')\right] B^\sigma_{n,\mathbf{k}}(\mathbf{G}), \tag{6}$$

where Ω is the supercell volume and $v_\alpha(q)$ is the Fourier transform of $v_\alpha(r)$. Previously impractical [15–19] calculations on large systems are enabled here by obtaining $W_\alpha(\mathbf{k})$ from

$$W_\alpha(\mathbf{k}) = \frac{1}{\Omega}\sum_\mathbf{R} W_\alpha(\mathbf{R})\, e^{i\mathbf{k}\cdot\mathbf{R}}, \tag{7}$$

and evaluating it via fast Fourier transformation (FFT). The evaluation of the Hamiltonian matrix elements requires $\propto (N_B \times N_\mathbf{k} \times N_G)^2$ operations, while the diagonalization of the matrix requires $\propto (N_B \times N_\mathbf{k})^3$ operations [here $N_B = (N_b, \sigma)$].

The dramatic reduction in the basis set size N_B and $N_\mathbf{k}$ afforded by the LCBB expansion is illustrated in Fig. 1, which shows the lowest three conduction bands of $(\mathrm{GaAs})_n/(\mathrm{AlAs})_n$ (001) superlattices versus the period n, as computed by the untruncated, "exact" plane-wave expansion of Eq. (1) (solid lines), and by successive truncations of N_B and $N_\mathbf{k}$ in the LCBB expansion (3) (dashed lines). We see [Fig. 1(a)] that using four valence bands and the two lowest conduction bands of GaAs and AlAs (so $N_B = 12$), and replacing the full reciprocal space $\mathbf{k} = (2\pi/na)\, j + \mathbf{k}_0$, $j \in [-n, n]$ by a limited grid of $j \in [-6, 6]$, $\mathbf{k}_0 = \Gamma$, and $j \in [-5, 5]$, $\mathbf{k}_0 = X$ (so $N_\mathbf{k} = 24$), we can reproduce all trends in the superlattice states (including the bendover at small n) within 2 meV down to the monolayer superlattice. Using the same $N_\mathbf{k}$ grid, but only a single band (the conduction band of GaAs for $\mathbf{k}_0 = \Gamma$ and the conduction band of AlAs for $\mathbf{k}_0 = X$, thus $N_B = 1$), the error is $\sim$10 meV for $n = 20$ ML [Fig. 1(b)] and the projections of the wave functions on the "exact" plane-wave result of Eq. (1) are 99.6% and 99.95% for the Γ and X states, respectively. We will use the latter N_B, $N_\mathbf{k}$ truncation in the following calculations.

Figure 2(a) shows the calculated pressure dependence of the transition energies from the valence-band maximum (VBM) to the $\bar{\Gamma}(\Gamma_{1c})$ and $\bar{\Gamma}(X_{1c})$ conduction bands in a $(\mathrm{GaAs})_{20}/(\mathrm{AlAs})_{20}$ superlattice. The coupling-induced *anticrossing* is evident. The Γ-X coupling matrix element $V_{\Gamma X}(n)$, obtained as one half of the minimum

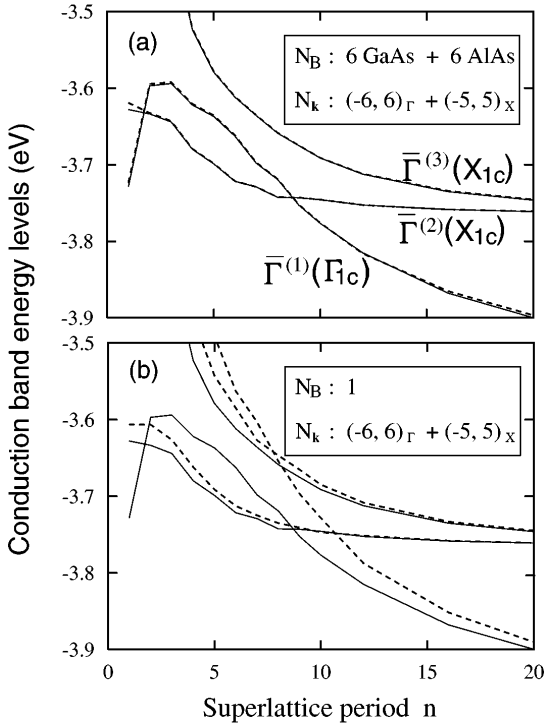

FIG. 1. Energy of the three lowest conduction states at the $\bar{\Gamma}$ point of (001) $(GaAs)_n/(AlAs)_n$ superlattices, obtained using different truncations (insets) in the number of bands N_B and the number of $\mathbf{k}$ points $N_\mathbf{k}$ in Eq. (3).

distance between the Γ and X curves, is 0.9 meV for $n = 20$. This value should be compared with 1.2 meV we obtained from an exact calculation (i.e., no truncation in N_B or $N_\mathbf{k}$). Figure 2(c) shows the VBM $\rightarrow$ CBM (conduction-band minimum) momentum transition matrix element $|\langle\psi_{\rm VBM}|\mathbf{p}|\psi_{\rm CBM}\rangle|^2$ as a function of pressure. We see that unlike alloys [3], the transition in superlattices (and dots) is *not* first order. The finite Γ-X coupling $V_{\Gamma X}$ leads to the presence of some Γ character even in the "indirect gap region" ($P \geq P_c$), producing there *a finite optical transition probability*.

In the above calculations we assumed ideal, sharp interfaces. To see whether interfacial roughness, present in real samples, can quench the Γ-X coupling, we have compared $V_{\Gamma X}$ for $(GaAs)_n/(AlAs)_n$ superlattices with sharp interfaces and with realistic segregated profiles obtained by solving the segregation equation [27]. The results (Fig. 3) show that while segregation reduces $V_{\Gamma X}$ by about a factor of 2, the odd-even oscillations of $V_{\Gamma X}$ with the period n are not washed out. In fact, while for *abrupt* SL's [Fig. 3(a)], $V_{\Gamma X} = 0$ for $n =$ odd, in segregated SL's, $V_{\Gamma X} \approx 0$ for $n =$ even [Fig. 3(b)]. Our calculated $V_{\Gamma X} = 1.24$ meV for a sharp $(GaAs)_{12}/(AlAs)_{28}$ SL, is in excellent agreement with the experimental [5] value of 1.25 meV.

We next study Γ-X coupling in GaAs dots embedded in AlAs matrix. To compare meaningfully the Γ-X coupling in quantum dots and superlattices, we have chosen a particular dot geometry (inset of Fig. 4): 20 monolayers (ML) of GaAs sandwiched by 20 ML of AlAs in the [001] direction and N ML of GaAs surrounded by 20 ML of AlAs in the [110] and $[1\bar{1}0]$ directions. Thus, when $N \rightarrow \infty$ the quantum dot merges into a 20×20 [001] superlattice. The pressure dependence of the transition energies and of the momentum matrix element for a $N = 140$ quantum dot are shown in Figs. 2(b) and 2(c) (where the supercell contains 2×10^6 atoms). The calculation takes $\sim$30 min on a IBM RS/6000 work station model 590 for one pressure value. We find that the Γ-X coupling in these QD's is *smaller* than in the corresponding 20×20 superlattice [compare Fig. 2(a)]. Furthermore, as shown in Fig. 4, the anticrossing gap $\Delta E_{\rm min}$ ($= 2V_{\Gamma X}$ in two level systems) in dots does not approach the superlattice value when N increases. There are two reasons for this: (i) For small dots, the 20 ML barrier region of AlAs in [110] and

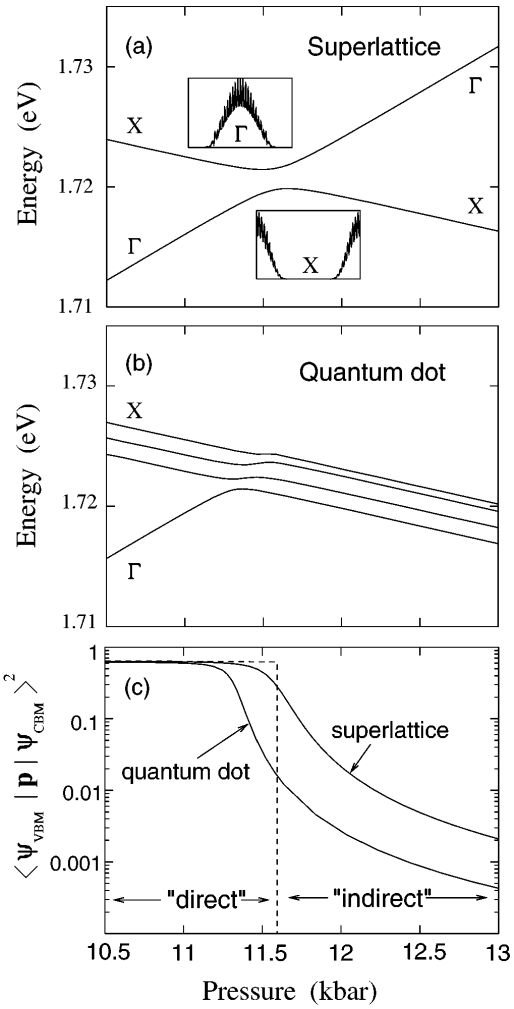

FIG. 2. Pressure dependence of the transition energies from the VBM to the Γ and X-derived conduction bands (a) and (b) and transition probabilities (c) of a $(GaAs)_{20}/(AlAs)_{20}$ superlattice and a $20 \times 140 \times 140$ quantum dot. The insets in part (a) show the Γ and X wave functions along the [001] direction of the superlattice. The dashed line in part (c) gives the SL transition probability expected in the absence of Γ-X coupling.

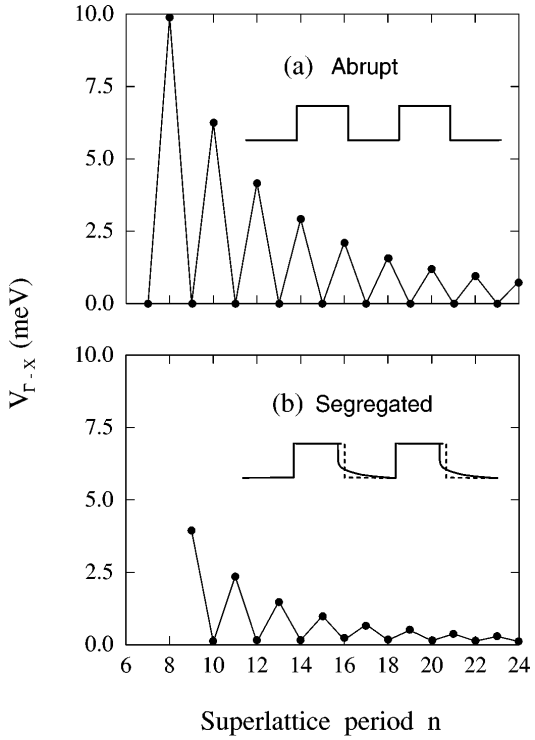

FIG. 3. Γ-X coupling matrix elements of abrupt (a) and segregated (b) $(GaAs)_n/(AlAs)_n$ [001] superlattices, as a function of the period n. These results are calculated without truncation on N_B and N_k.

$[1\bar{1}0]$ directions reduces the ratio between the area of the $N \times N$ GaAs (001) interface and the total volume of AlAs [compared to the $(GaAs)_{20}/(AlAs)_{20}$ SL]. This reduces the Γ-X coupling. (ii) For a dot with large N, there are multiple X states with energy separation comparable to $V_{\Gamma X}$ which can couple with each other [see Fig. 2(b)];

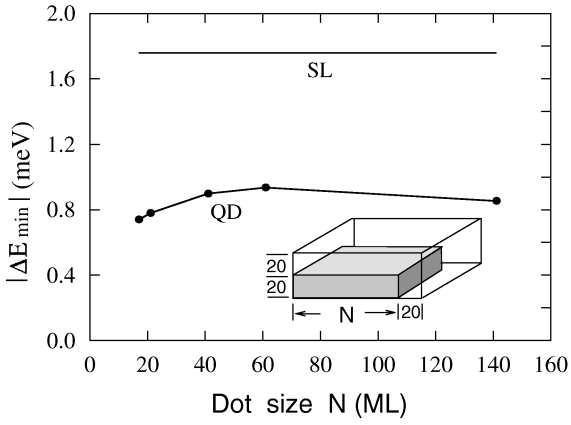

FIG. 4. Γ-X level splitting at the pressure-induced Γ-X transition in GaAs/AlAs quantum dots of size $20 \times N \times N$ ML, as a function of N. The level splitting of a 20×20 superlattice is also shown for comparison.

the lowest X state is repelled both from above and below, reducing the anticrossing gap.

To test the generality of the conclusion that $V_{\Gamma X}$ is smaller in a quantum dot than in a superlattice of comparable size, we compared the $2V_{\Gamma X}$ of $n \times n \times n$ ML Ga-centered (100) $\times$ (010) $\times$ (001) cubic GaAs quantum dots (embedded in $2n \times 2n \times 2n$ AlAs supercells) with $(GaAs)_n/(AlAs)_n$ superlattices. We found $2V_{\Gamma X}$ of 0.76, 4.6 meV for $n = 24, 10$ quantum dots, smaller than the 0.98, 9.6 meV results of the corresponding superlattices.

In conclusion, we find that the Γ-X coupling (anticrossing) in quantum dot is always smaller than the coupling in the comparable superlattice. This result conflicts with the common wisdom expectation that quantum confinement effects diminish in going from a 0D quantum dot to a 1D quantum wire and to a 2D quantum well. The reduced anticrossing in large dots is partially due to the existence of a complex pattern of Γ-X coupling leading to partially canceling upwards and downwards level repulsions.

This work was supported by the U.S. Department of Energy, OER-BES, under Grant No. DE-AC36-83CH10093.

[1] B. Welber *et al.*, Phys. Rev. B **12**, 5729 (1975).
[2] H. Müller *et al.*, Phys. Rev. B **21**, 4879 (1980).
[3] B. Koiller and R. B. Capaz, Phys. Rev. Lett. **74**, 769 (1995).
[4] A. Onton and R. J. Chicotka, Phys. Rev. B **4**, 1847 (1971).
[5] M. H. Meynadier *et al.*, Phys. Rev. Lett. **60**, 1338 (1988).
[6] N. J. Pulsford *et al.*, Phys. Rev. Lett. **63**, 2284 (1989).
[7] M. Nakayama *et al.*, Solid State Commun. **88**, 43 (1993).
[8] V. Voliotis *et al.*, Phys. Rev. B **49**, 2576 (1994).
[9] M. Holtz, *et al.*, Phys. Rev. B **41**, 3641 (1990).
[10] G. H. Li *et al.*, J. Phys. Chem. Solids **56**, 385 (1995); Phys. Rev. B **50**, 18 420 (1994).
[11] A. Franceschetti and A. Zunger, Phys. Rev. B **52**, 14 664 (1995).
[12] L. J. Sham and Y. T. Lu, J. Lumin. **44**, 207 (1989).
[13] E. L. Ivchenko *et al.*, Solid State Electron. **37**, 813 (1994).
[14] M. G. Burt, J. Phys. Condens. Matter **4**, 6651 (1992).
[15] D. Z. Ting and Y. C. Chang, Phys. Rev. B **36**, 4359 (1987).
[16] J. N. Schulmann *et al.*, Phys. Rev. B **31**, 2056 (1985).
[17] M. A. Gell *et al.*, J. Phys. C **19**, 3821 (1986).
[18] I. Morrison *et al.*, Phys. Rev. B **42**, 11 818 (1990); K. B. Wong *et al.*, Phys. Rev. B **35**, 2463 (1987).
[19] J. B. Xia, Surf. Sci. **228**, 476 (1989).
[20] R. G. Dandrea and A. Zunger, Phys. Rev. B **43**, 8962 (1991).
[21] S. H. Wei and A. Zunger, J. Appl. Phys. **63**, 5794 (1988).
[22] S. Froyen, J. Phys. Condens. Matter **8**, 11 029 (1996).
[23] D. M. Wood and A. Zunger, Phys. Rev. B **53**, 7949 (1996).
[24] L. W. Wang and A. Zunger, Phys. Rev. B **54**, 11 417 (1996).
[25] J. P. Cuypers *et al.*, Phys. Rev. B **48**, 11 469 (1993).
[26] Y. Fu *et al.*, Phys. Rev. B **47**, 13 498 (1993).
[27] G. S. Spencer *et al.*, Phys. Rev. B **52**, 8205 (1996).